JOURNAL OF AGRICULTURAL AND FOOD CHEMISTRY

Color Properties of Four Cyanidin–Pyruvic Acid Adducts

JOANA OLIVEIRA,[†] VIRGÍNIA FERNANDES,[†] CÁNDIDA MIRANDA,[‡] CELESTINO SANTOS-BUELGA,[§] ARTUR SILVA,[||] VICTOR DE FREITAS,[†] AND NUNO MATEUS*,[†]

Centro de Investigação em Química, Departamento de Química, Faculdade de Ciências, Universidade do Porto, Rua do Campo Alegre, 687, 4169-007 Porto, Portugal, FRULACT, S. A. Rua do Outeiro, 589, 4475-150 Gemunde Maia, Portugal, Departamento de Química, Universidade de Aveiro, 3810-193 Aveiro, Portugal, and Unidad de Nutrición y Bromatología, Facultad de Farmacia, Universidad de Salamanca, Campus Miguel de Unamuno s/n, E-37007 Salamanca, Spain

Four anthocyanin−pyruvic adducts were synthesized through the reaction of cyanidin 3-*O*-glucoside, cyanidin 3-*O*-rutinoside, cyanidin 3-*O*-sophoroside, and cyanidin 3-*O*-sambubioside with pyruvic acid, structurally characterized by liquid chromatography−mass spectrometry (LC−MS) and nuclear magnetic resonance (NMR), and their chromatic properties were studied (pH and SO_2 stability assays). Overall, these pigments were shown to have a higher resistance to discoloration toward pH variations and also in the presence of SO_2, being that this resistance to discoloration was explained by a higher protection of the chromophore group against the water or bisulfite nucleophilic attack that gives rise to the colorless hemiacetal form. Only slight differences in the protection against the nucleophilic attack of water and bisulfite were found to occur between all of the cyanidin−pyruvic acid adducts studied. Indeed, anthocyanin−pyruvic acid adducts with glucose or sambubiose attached to the 3-O position of the flavylium moiety were shown to have smaller bleaching constants compared with similar pigments that possess a rutinosyl or sophorosyl moiety. The study of the pigments (A−D and cyanidin-3-*O*-glucoside) color parameters, namely, chroma (C^*), lightness (L^*), and the hue angle ($h_{a,b}$), obtained from the CIELAB system, revealed that different patterns of sugars in the anthocyanin−pyruvic acid adduct moiety affected the referred three parameters of color. The loss of saturation ($\Delta C^* < 0$) and the increase of lightness ($\Delta L^* > 0$) presented by the cyanidin−pyruvic acid adduct solutions at acidic pH values (1.0 and 2.0) showed that they are much less colored than the cyanidin-3-*O*-glucoside. For higher pH values (5.0 and 7.0), the reverse trend was observed. This means that the cyanidin−pyruvic acid adducts A−D are much more colored than the anthocyanin at these pH values. The higher coloring capacity of these pigments at higher pH values may be an important feature, indicating a putative application of these compounds in food products.

KEYWORDS: Cyanidin−pyruvic acid adducts; red fruit extracts; NMR; color stability; pH; bisulfite; CIELAB

INTRODUCTION

Anthocyanins constitute a major polyphenolic family of compounds widespread in the plant kingdom and are responsible for the color of a large number of flowers and fruits. These compounds are of interest for the food industry because they may have some applications as natural food colorants. The natural pigments give rise to different colors from red−blue to orange, depending upon their structure and the pH of the medium (*1*, *2*). In aqueous solution, anthocyanins exist in different forms in equilibrium. In very acidic aqueous solutions (pH < 1), they occur as red flavylium cations. In aqueous media, increasing the pH leads to a reduction of the intensity of the color because of a decrease in the concentration of the flavylium cation that is converted into its colorless hemiacetal form by the nucleophilic attack of water. At low acidic, neutral, and basic pH values, deprotonation of the flavylium cation also occurs, giving rise to the violet/blue quinoidal forms, although this reaction is very limited in aqueous solutions (*1*). These color changes represent a disadvantage for their use as colorants in food matrixes in which the pH conditions are near neutrality and different from those of the maximum color expression of the anthocyanins. Therefore, research groups from the food industry have been searching for new natural pigments with increased stability to pH, SO_2, temperature, etc.

Young red wines are usually rich in anthocyanins, which are the main compounds responsible for their color. During wine

* To whom correspondence should be addressed. E-mail: nbmateus@fc.up.pt. Fax: +351-226082959. Telephone: +351-226082858.
[†] Centro de Investigação em Química.
[‡] FRULACT, S. A.
[§] Universidad de Salamanca.
[||] Universidade de Aveiro.

10.1021/jf061085b CCC: $33.50
Published on Web 08/03/2006

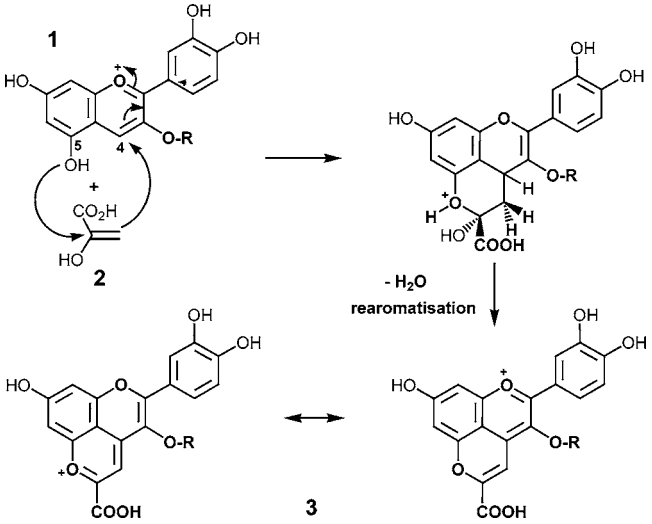

Figure 1. Mechanism for the formation of cyanidin–pyruvic acid adducts: cyanidin-3-*O*-glycoside, 1; pyruvic acid, 2; and cyanidin-3-*O*-glycoside–pyruvic acid adducts, 3; R = glycosyl moiety.

aging, these anthocyanins are progressively displaced by newly formed pigments (*3*−*5*). These new pigments were initially thought to arise mainly from direct condensation between anthocyanins and catechins (*6*−*10*). A few years ago, new classes of anthocyanin-derived pigments, described as pyranoanthocyanins were found to occur in red wines (*11*−*17*). One of the most important pyranoanthocyanin groups is that comprising the anthocyanin−pyruvic acid adducts, which results from the cyclic addition of pyruvic acid onto carbon 4 and an hydroxyl group at the carbon 5 position of the anthocyanin (**Figure 1**), yielding a fourth ring, which is thought to be responsible for a higher stability compared to the original anthocyanins (*11*, *12*). These new pigments were also found to be more resistant to bleaching by sulfur dioxide (*11*, *18*−*20*). These compounds showed a UV/vis spectra difference with a λ_{max} hypsochromically shift compared to that of the anthocyanins, conferring on them a red/orange color (*11*−*13*). The interest in anthocyanin−pyruvic acid adducts goes beyond wine chemistry. The chromatic properties of this kind of pigment brings expectations concerning the use of these natural pigments in the food industry. Bearing this in mind, the aim of this work was to synthesize different anthocyanin−pyruvic acid adducts from the reaction of pyruvic acid with several anthocyanins, varying only in the structure of the sugar moiety, obtained from several red fruits. These compounds were structurally and chromatically characterized to better understand their stability properties, especially their resistance to discoloration.

MATERIALS AND METHODS

Reagents. TSK Toyopearl gel HW-40(S) was purchased from Tosoh (Tokyo, Japan); pyruvic acid (d = 1.267; 97%) was purchased from Sigma-Aldrich (Madrid, Spain).

Extracts Preparation. A total of 1 kg of blackberries (*Rubus fruticosus*), sweet cherries (*Prunus avium*), raspberries (*Rubus idaeus*), and elderberries (*Sambucus nigra*) was extracted with a solution of 50% aqueous ethanol (pH 1.5, acidified with HCl) for 1 day at room temperature. The anthocyanin extracts were purified by a TSK Toyopearl gel column (250 × 16 mm i.d.) chromatography according to the procedure described previously (*21*).

Synthesis of Anthocyanin−Pyruvic Acid Adducts. The synthesis of anthocyanin−pyruvic acid adducts was obtained through the reaction of anthocyanin extracts with pyruvic acid. Anthocyanins (312.5 μM) were incubated in 1 L of water at pH 2.6 and at 35 °C with pyruvic acid (pyruvic acid/anthocyanin molar ratio of 50:1). The formation of the new pigments was monitored by high-performance liquid chromatography (HPLC) with diode array detection (DAD). After 5 days, the reactions were stopped and the major compounds were purified.

Purification of Anthocyanin−Pyruvic Acid Adducts. Each reaction mixture of the pigments was applied directly onto a 250 × 16 mm i.d. TSK Toyopearl gel HW-40(S) column, with the anthocyanin−pyruvic acid adducts fractions being eluted with 20% ethanol in water. The pigments collected were submitted to semipreparative HPLC using the conditions described below. The isolated pigments were then submitted to further purification, which consisted of a final elution on silica gel 100 C18 reversed phase using a vacuum filtration system.

HPLC Analysis. All of the extracts were analyzed by Knauer K-1001 HPLC on a 250 × 4.6 mm i.d. reversed-phase C18 column (Merck, Darmstadt, Germany); detection was carried out at 520 nm using a Knauer K-2800 diode array detector. The solvents were A, H_2O/HCOOH (9:1), and B, H_2O/CH_3CN/HCOOH (6:3:1). The gradient consisted of 20−85% of B for 70 min at a flow rate of 1.0 mL/min. The column was washed with 100% of B for 20 min and then stabilized with the initial conditions during another 20 min.

LC−MS Analysis. A Hewlett-Packard 1100 series liquid chromatograph, equipped with a 150 × 4.6 mm i.d., 5 μm AQUA (Phenomenex, Torance, CA) reversed-phase C18 column, thermostatted at 35 °C, was used. Solvents were A, aqueous 0.1% trifluoroacetic acid, and B, acetonitrile, with the gradient reported previously (*21*). The capillary voltage was 3 V, and the capillary temperature was 190 °C. Spectra were recorded in positive-ion mode between *m*/*z* 120 and 1500. The mass spectrometer was programmed to do a series of three scans: a full mass, a zoom scan of the most intense ion in the first scan, and a MS−MS of the most intense ion using relative collision energy of 30 and 60.

Nuclear Magnetic Resonance (NMR). ^{1}H NMR (500.13 MHz) and ^{13}C NMR (125.77 MHz) spectra were measured in CD_3OD/trifluoroacetic acid (TFA) (98:2) on a Bruker-Avance 500 spectrometer at 303 K and with tetramethylsilane (TMS) as an internal standard. ^{1}H chemical shifts were assigned using 1D and 2D ^{1}H NMR [*g* correlation spectroscopy (COSY) and nuclear Overhauser effect spectrometry (NOESY)], while ^{13}C resonances were assigned using 2D NMR techniques [*g* heteronuclear multiple-bond correlation (HMBC) and *g* heteronuclear single-quantum coherence (HSQC)] (*22*, *23*). The delay for the long-range C/H coupling constant was optimized to 7 Hz.

pH Assay. For the pH assay, solutions of each pigment (2 mM) were prepared in 12% (v/v) aqueous ethanol and added to buffer solutions with different pH values in a range between 1.0 and 11.0. The solvents used for preparations of the buffer solutions were 0.2 M KCl, 0.2 M HCl, 0.1 M $KHC_8O_4H_4$, 0.1 M HCl, 0.1 M NaOH, 0.1 M KH_2PO_4, 0.1 M tris-(hydroxymethyl)-aminomethane, 0.025 M Borax, and 0.05 M Na_2HPO_4 according to Robinson and Stokes (*24*), where the final concentration of each pigment was 0.08 mM. All of the pigments solutions were left to equilibrate for 2 h, and then spectroscopic absorbance curves were recorded for all of the solutions from 360 to 830 nm with a 1 nm sampling interval, using a 10 mm path-length cell in a Shimadzu UV-3101 spectrophotometer.

SO_2 Assay. The bleaching by SO_2 was studied using the pigment solution with pH 2.0. To this solution were added different aliquots of an aqueous solution of sodium bisulfite to achieve SO_2 concentrations in the range between 0 and 200 ppm. Spectroscopic absorbance curves were recorded for all of these solutions from 360 to 830 nm with a 1 nm sampling interval, using a 10 mm path-length cell in a Shimadzu UV-3101 spectrophotometer. The bleaching constant (K_{SO_2}) was calculated from the slope of the graphic of the color intensity curve of absorbance (at the λ_{max} of each pigment) as a function of the concentration of SO_2.

L*, a*, b* **CIELAB Color Measurements.** Spectroscopic curves of the solutions of the pigments at pH values 1.0, 2.0, 5.0, and 7.0 were recorded from 360 to 830 nm with a 1 nm sampling interval, using a 2 mm path-length cell in a Shimadzu UV-3101 spectrophotometer. The color coordinates were determined in the CIELAB color space using CIE D65/10° illuminant/observer conditions (*25*). All of the color calculations were performed using a computer program developed at the Physics Department of the University of Porto, Portugal. Tristimulus values were used to calculate the CIELAB

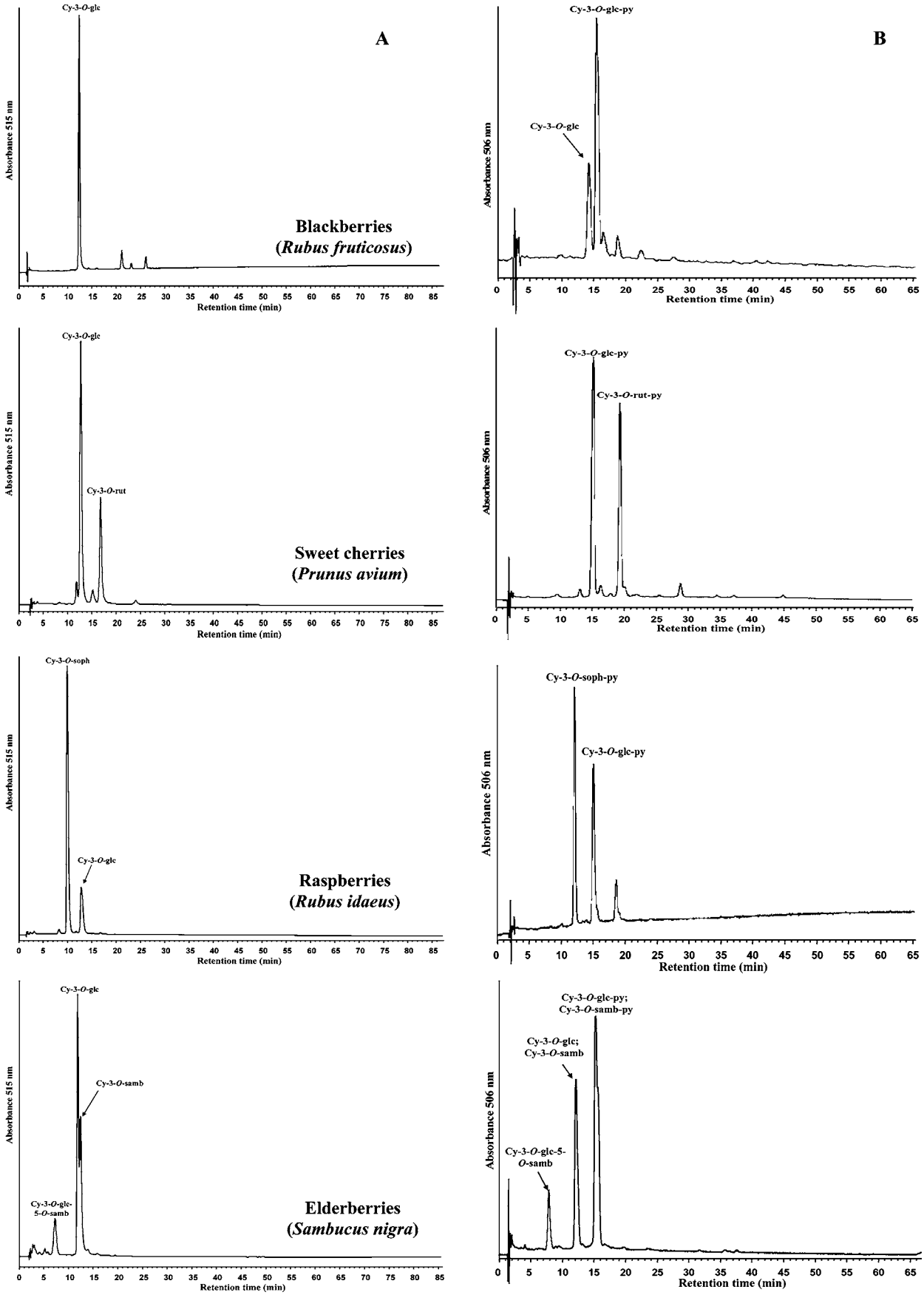

Figure 2. HPLC chromatograms recorded at (A) 515 nm of the anthocyanin extracts (blackberries, sweet cherries, raspberries, and elderberries) and (B) 506 nm of the synthesis of cyanidin–pyruvic acid adducts from the reaction between pyruvic acid and different anthocyanin extracts: Cy, cyanidin; Glc, glucose; Rut, rutinose; Soph, sophorose; Samb, sambubiose; py, pyruvic acid adducts.

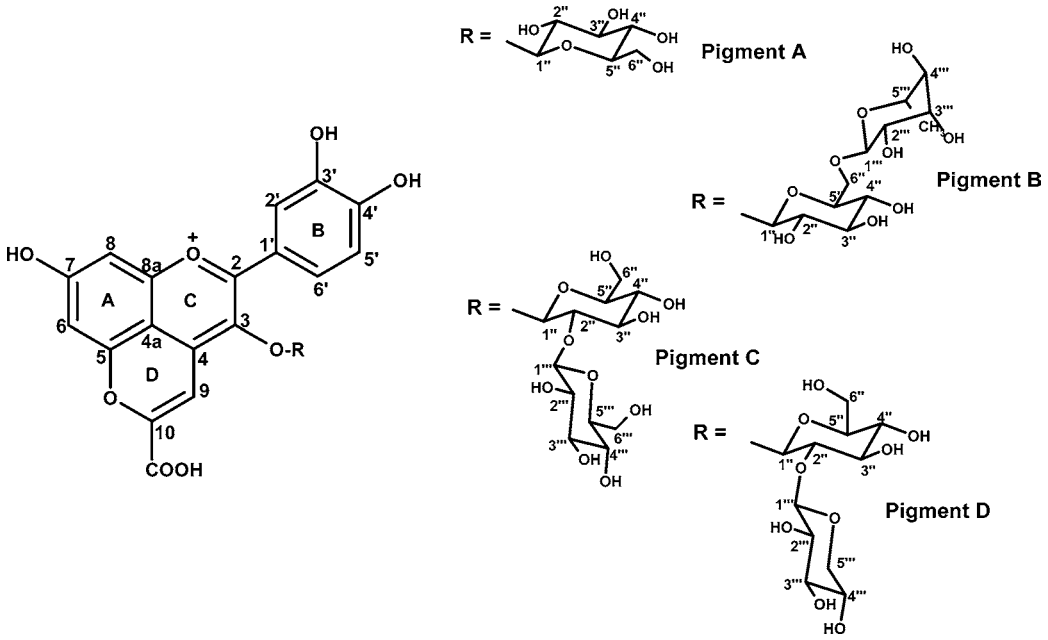

Figure 3. Structure of the synthesized cyanidin–pyruvic acid adducts: A, cyanidin-3-*O*-glucoside–pyruvic acid adduct; B, cyanidin-3-*O*-rutinoside–pyruvic acid adduct; C, cyanidin-3-*O*-sophoroside–pyruvic acid adduct; D, cyanidin-3-*O*-sambubioside–pyruvic acid adduct.

coordinates (L^*, a^*, and b^*). Besides L^* (correlate of lightness), the psychophysical color parameters chroma (C^*, correlate of saturation) and hue angle ($h_{a,b}$, correlate of hue) were obtained by the transformation of the Cartesian coordinates (a^* and b^*) to polar coordinates (C^* and $h_{a,b}$), according to Gonnet (*26*). L^* means lightness to darkness ($+L$ or $-L$); $+a$ means redness to greenness $-a$; and $+b$ means yellowness to blueness $-b$. Other parameters were C^*, chroma, ranging from neutral to fully saturated color ($+C$ or $-C$), and h, the hue angle of the color change around the color circle ($+h$ or $-h$).

To allow for a better correlation between "visual" and "colorimetric" differences, the colorimetric difference ΔE^* and its components ΔL^*, ΔC^*, ΔH^*, and $\Delta h_{a,b}$ for each sample pair (sample and reference) were obtained through the equations: $\Delta E^* = [(\Delta L^*)^2 + (\Delta a^*)^2 + (\Delta b^*)^2]^{0.5}$; $\Delta L^* = L^*_{sample} - L^*_{reference}$; $\Delta C^* = C^*_{sample} - C^*_{reference}$; $\Delta H^* = 2\sin(\Delta h/2)(C^*_{sample} - C^*_{reference})^{0.5}$; and $\Delta h_{a,b} = h_{a,b\ sample} - h_{a,b\ reference}$. The colorimetric difference ΔE^* reveals the changes in all colorimetric parameters such as chroma, lightness, and tonality, and a mean threshold

Table 1. ^{1}H and ^{13}C Chemical Shifts of Cyanidin-3-*O*-Glucoside–Pyruvic Acid Adduct (Pigment A), Determined in CD_3OD/TFA (98:2)[a]

position	δ ^{1}H (ppm); *J* (Hz)	δ ^{13}C	HMBC	HSQC
pyranocyanidin moiety				
2		166.0	H-2′, H-6′	
3		137.0	H-9, H-1″	
4		na		
4a		110.7	H-6, H-8	
5		154.3	H-6	
6	7.15; d, 1.8	103.0		H6
7		169.4	H-6, H-8	
8	7.23; d, 1.8	102.0		H-8
8a		154.3	H-8	
9	7.99; s	107.5		H-9
10		155.7	H-9	
COOH		161.3	H-9	
1′		121.2	H-5′	
2′	7.81; d, 2.2	117.7		H-2′
3′		147.2	H-5′	
4′		147.2	H-2′, H-6′	
5′	6.93; d, 8.6	116.8		H-5′
6′	8.04; dd, 8.6/2.2	127.4		H-6′
glucose moiety				
1″	4.69; d, 7.7	105.7		H-1″
2″	3.63; dd. 9.2/7.7	75.3		H-2″
3″	3.37*	77.6		H-3″
4″	3.13*	71.4		H-4″
5″	3.15–3.17; m	77.8		H-5″
6a″	3.73; dd, 11.6/1.8	62.7		H-6a″, H-6b″
6b″	3.39; dd, 11.6/6.2	62.7		H-6a″, H-6b″

[a] Key: *, unresolved; s, singlet; d, doublet; dd, double doublet; m, multiplet; na, not assigned.

Table 2. ^{1}H and ^{13}C Chemical Shifts of Cyanidin-3-*O*-Rutinoside–Pyruvic Acid Adduct (Pigment B), Determined in CD_3OD/TFA (98:2)[a]

position	δ ^{1}H (ppm); *J* (Hz)	δ ^{13}C	HMBC	HSQC
pyranocyanidin moiety				
2		166.4	H-2′, H-6′	
3		136.2	H-9, H-1″	
4		110.7	H-9	
4a		110.7	H-6, H-8	
5		154.5	H-6	
6	7.16; d, 1.9	100.8		H-6
7		169.8	H-6, H-8	
8	7.24; d, 1.9	100.1		H-8
8a		154.3	H-8	
9	8.03; s	105.6		
10		155.6	H-9	
COOH		161.4	H-9	
1′		121.5	H-5′	
2′	7.89; d, 2.1	116.8		H-2′
3′		146.7	H-5′	
4′		147.2	H-2′, H-6′	
5′	7.00; d, 8.6	115.6		H-5′
6′	8.08; dd, 8.6/2.1	125.5		H-6′
rutinose moiety				
1″	4.67; d, 7.7	103.8		H-1″
2″	3.65, dd, 9.2/7.7	73.3		H-2″
3″	3.36*	75.8		H-3″
4″	3.78*	66.5		H-4″
5″	3.93–3.95, m	81.5		H-5″
6a″	4.08, dd, 11.3/1.4	65.9		H-6a″, H-6b″
6b″	3.60*	65.9		H-6a″, H-6b″
1‴	4.37; br s	100.7		H-1‴
2‴	3.45, dd, 3.1/1.5	70.2		H-2‴
3‴	3.27*	70.9		H-3‴
4‴	3.16*	71.5		H-4‴
5‴	3.26*	70.2		H-5‴
CH_3	1.10; d, 6.1	16.2		CH_3

[a] Key: *, unresolved; s, singlet; d, doublet; dd, double doublet; m, multiplet; br s, broad singlet.

Table 3. ^{1}H and ^{13}C Chemical Shifts of Cyanidin-3-*O*-Sophoroside–Pyruvic Acid Adduct (Pigment C), Determined in CD_3OD/TFA (98:2)[a]

position	δ ^{1}H (ppm); *J* (Hz)	δ ^{13}C	HMBC	HSQC
pyranocyanidin moiety				
2		166.8	H-2′, H-6′	
3		135.6	H-9, H-1″	
4		110.7	H-9	
4a		110.7	H-6, H-8	
5		154.5	H-6	
6	7.16; d, 1.9	101.2		H-6
7		169.4	H-6, H-8	
8	7.24; d, 1.9	100.9		H-8
8a		154.5	H-8	
9	8.08; s	107.3		H-9
10		154.9	H-9	
COOH		161.4	H-9	
1′		117.1	H-5′	
2′	8.00; d, 2.2	118.5		H-2′
3′		146.5	H-5′	
4′		146.5	H-2′, H-6′	
5′	6.99; d, 9.1	116.8		H-5′
6′	8.00; dd, 9.1/2.2	126.6		H-6′
sophorose moiety				
1″	4.71; d, 7.7	103.3		H-1″
2″	3.94*	83.0		H-2″
3″	3.57; t, 9.1	77.2		H-3″
4″	3.30*	70.5		H-4″
5″	3.38*	77.6		H-5″
6a″	3.74; dd, 11.8/2.9	61.7		H-6a″, H-6b″
6b″	3.91; dd, 11.8/1.4	61.7		H-6a″, H-6b″
1‴	4.86; d, 7.1	105.6		H-1‴
2‴	3.48*	75.2		H-2‴
3‴	3.38*	77.6		H-3‴
4‴	3.19*	70.5		H-4‴
5‴	3.90*	77.9		H-5‴
6a‴	3.74*	61.6		H-6a‴, H-6b‴
6b‴	3.35*	61.6		H-6a‴, H-6b‴

[a] Key: *, unresolved; s, singlet; d, doublet; dd, double doublets; t, triplet.

Table 4. ^{1}H and ^{13}C Chemical Shifts of Cyanidin-3-*O*-Sambubioside–Pyruvic Acid Adduct (Pigment D), Determined in CD_3OD/TFA (98:2)[a]

position	δ ^{1}H (ppm); *J* (Hz)	δ ^{13}C	HMBC	HSQC
pyranocyanidin moiety				
2		166.1	H-2′, H-6′	
3		135.9	H-9, H-1″	
4		110.6	H-9	
4a		110.8	H-6, H-8	
5		153.9	H-6	
6	7.14; br s	101.8		H-6
7		169.4	H-6, H-8	
8	7.22; br s	101.1		H-8
8a		154.1	H-8	
9	8.07; s	107.4		H-9
10		155.3	H-9	
COOH		161.3	H-9	
1′		121.1	H-5′	
2′	8.08; d, 2.1	118.0		H-2′
3′		146.9	H-5′	
4′		144.6	H-2′, H-6′	
5′	6.92; d, 8.8	116.6		H-5′
6′	8.08; dd, 8.8/2.1	127.2		H-6′
sambubiose moiety				
1″	4.78; d, 7.7	103.2		H-1″
2″	3.88*	82.7		H-2″
3″	3.57, t, 9.2	77.8		H-3″
4″	3.28*	70.7		H-4″
5″	3.17–3.19, m	78.5		H-5″
6a″	3.71*	62.3		H-6a″, H-6b″
6b″	3.38*	62.3		H-6a″, H-6b″
1‴	4.69; d, 7.7	105.3		H-1‴
2‴	3.64*	75.0		H-2‴
3‴	3.38*	77.1		H-3‴
4‴	3.19*	78.5		H-4‴
5a‴	3.60*	70.5		H-5a‴, H-5b‴
5b‴	3.27*	70.5		H-5a‴, H-5b‴

[a] Key: *, unresolved; br s, broad singlet; s, singlet; d, doublet; dd, double doublets; t, triplet; m, multiplet.

value of $\Delta E^* = 1$ is assumed as a basis for perceptible color differences between two solutions (*27*).

RESULTS AND DISCUSSION

Anthocyanins were obtained from different red fruit extracts. The anthocyanin profile of these extracts was determined by HPLC/DAD−MS and showed that the major anthocyanin pigments were cyanidin-based (**Figure 2A**). These anthocyanin profiles were already anticipated as the red fruits were chosen aiming to obtain the same anthocyanin with different types of sugar linked to the 3-O position of anthocyanin ring C (*28*−*32*). Bearing this in mind, these anthocyanin extracts were used to produce the respective anthocyanin−pyruvic acid adducts, namely, four major pigments: A, cyanidin-3-*O*-glucoside−pyruvic adduct; B, cyanidin-3-*O*-rutinoside−pyruvic adduct; C, cyanidin-3-*O*-sophoroside−pyruvic adduct; and D, cyanidin-3-*O*-sambubioside−pyruvic adduct. These pigments were synthesized in model solutions through the reaction of the anthocyanin extracts with pyruvic acid. The formation of the anthocyanin−pyruvic adducts after 5 days of the reaction is illustrated in the chromatograms shown in **Figure 2B**. These pigments were isolated by semipreparative HPLC and structurally characterized by HPLC/DAD−MS and 1D and 2D NMR analysis. Their chromatic properties, namely, their color stability toward discoloration by pH and bisulfite were also studied. The influence of the nature of the sugar attached to the pyranoanthocyanin moiety on the color parameters was assessed through analysis with the CIELAB system.

Structural Analysis. Pigment A analyzed by HPLC/DAD−MS was found to correspond to the cyanidin-3-*O*-glucoside−pyruvic acid adduct, as shown in **Figure 3**. The MS data of the pigment detected produced a $[M]^+$ ion at *m*/*z* 517 and a fragment ion $[M-162]^+$ at *m*/*z* 355 corresponding to the loss of the glucosyl moiety.

The structure of this compound was elucidated by NMR analysis (**Table 1**).

The protons H-6 and H-8 of ring A were assigned to two doublets with a small coupling constant ($J = 1.8$ Hz) at 7.15 and 7.23 ppm, respectively. The proton H-2′ was assigned to a small doublet ($J = 2.2$ Hz) at 7.81 ppm. The proton H-6 was assigned to a double doublet ($J = 8.6/2.2$ Hz) at 8.04 ppm. The proton H-5′ was attributed to a doublet ($J = 8.6$ Hz) at 6.93 ppm. The proton H-9 was located at 7.99 ppm. With respect to the glucosyl moiety, the anomeric proton was assigned to the doublet ($J = 7.7$ Hz) at 4.69 ppm. The proton H-2″ was attributed to a double doublet ($J = 9.2/7.7$ Hz) at 3.63 ppm. Proton H-5″ was assigned to the multiplet at 3.15 ppm. Protons H-6a″ and H-6b″ were attributed to the double doublets ($J =$ 11.6/1.8 and 11.6/6.2 Hz, respectively) at 3.73 and 3.39 ppm. The glucosyl protons H-3″ and H-4″ were situated in the 3.13−3.37 ppm region.

The assignment of the carbon resonances was possible using two-dimensional techniques (HSQC and HMBC). Carbons C-6, C-8, C-2′, C-5′, C-6′, and C-9 were assigned at 103.0, 102.0, 117.7, 116.8, 127.4, and 107.5 ppm, respectively, by their direct ^{1}H−^{13}C correlations with protons H-6, H-8, H-2′, H-5′, H-6′, and H-9. Carbon C-4′ of ring B was assigned by its long-distance correlation with protons H-2′ and H-6′ from the same ring. C-10 was assigned at 155.7 ppm through its HMBC correlations with H-9. Carbons C-4a and C-7 were determined from its long-

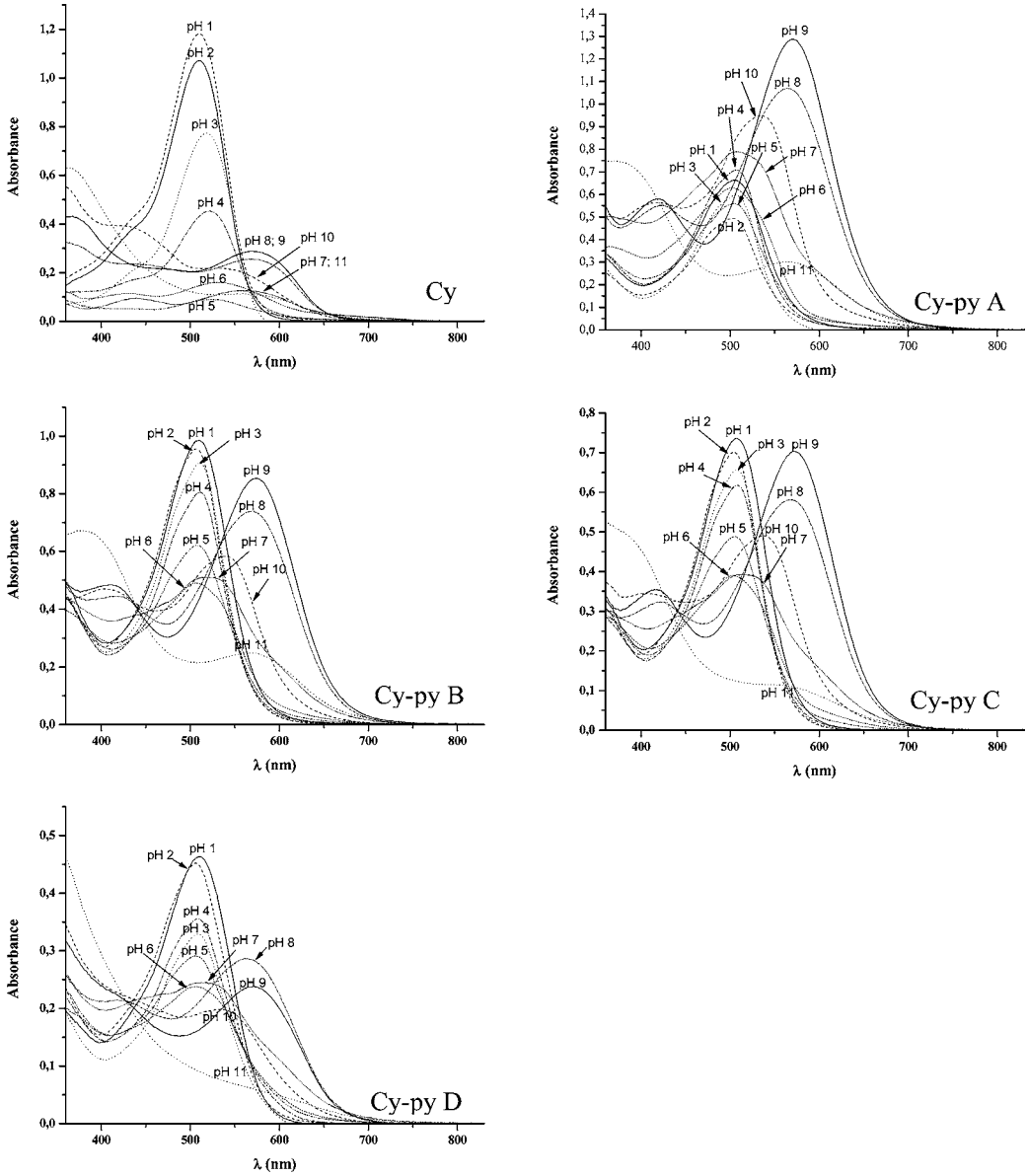

Figure 4. UV/vis spectra of cyanidin-3-*O*-glucoside (Cy-3-glc) and cyanidin–pyruvic acid adducts (Cy-py) A–D at different pH values (1.0–11.0).

range couplings with H-6 and H-8. The quaternary carbons C-5 and C-8a were assigned from the long-distance correlation with proton H-6 and H-8, respectively. The quaternary carbon C-2 was assigned from the long-distance correlation with protons H-2′, H-6′, and carbon C-3 was assigned from the correlation with protons H-9 and H-1″. All of the carbons of the glucosyl moiety were assigned through direct $^{1}H-^{13}C$ correlations in the HSQC spectrum.

Pigment B was found to correspond to the cyanidin-3-*O*-rutinoside−pyruvic acid adduct, as shown in **Figure 3**. The MS data of the pigment detected produced a $[M]^+$ ion at *m*/*z* 663 and a fragment ion $[M-308]^+$ at *m*/*z* 355 corresponding to the loss of the rutinosyl moiety. The structure of this anthocyanin−pyruvic acid adduct was attributed by NMR analysis (**Table 2**), similar to the analysis of pigment A. The major differences concerned the sugar moiety.

Rutinose is composed by a molecule of glucose linked to a molecule of rhamnose by a α-(*1*,*6*) linkage. With respect to the glucosyl moiety, the anomeric proton was assigned to the doublet ($J = 7.7$ Hz) at 4.67 ppm. All of the other glucosyl protons were situated in the 3.36−3.93 ppm region, except for the last two protons H-6a″ and H-6b″ that were assigned at 4.08 and 3.60 ppm, respectively. This suggests that the rhamnosyl moiety is linked to C-6 of the glucosyl moiety. The broad singlet at 4.37 ppm corresponds to the anomeric proton of the rhamnosyl moiety. The small coupling constant suggests a α configuration of the rhamnose molecule. Protons of the rhamnosyl moiety were situated in the 3.16−3.45 ppm region. The methyl group of the rhamnose was assigned to a doublet ($J = 6.1$ Hz) at 1.10 ppm. All of the carbons of the rutinosyl moiety were assigned through direct $^{1}H-^{13}C$ correlations in the HSQC spectrum.

Pigment C was found to correspond to the cyanidin-3-*O*-sophoroside−pyruvic acid adduct, as shown in **Figure 3**. The MS data of the pigment detected produced a $[M]^+$ ion at *m*/*z* 679 and a fragment ion $[M-324]^+$ at *m*/*z* 355 corresponding to the loss of the sophorosyl residue.

The structure of this anthocyanin−pyruvic acid adducts was attributed by NMR analysis (**Table 3**), similar to the analysis of pigments A and B. The major differences concerned the sugar moiety.

Sophorose is composed by two molecules of glucose linked by a *β*-(*1*,*2*) linkage. With respect to the glucosyl moiety linked directly to the anthocyanin, the anomeric proton was assigned

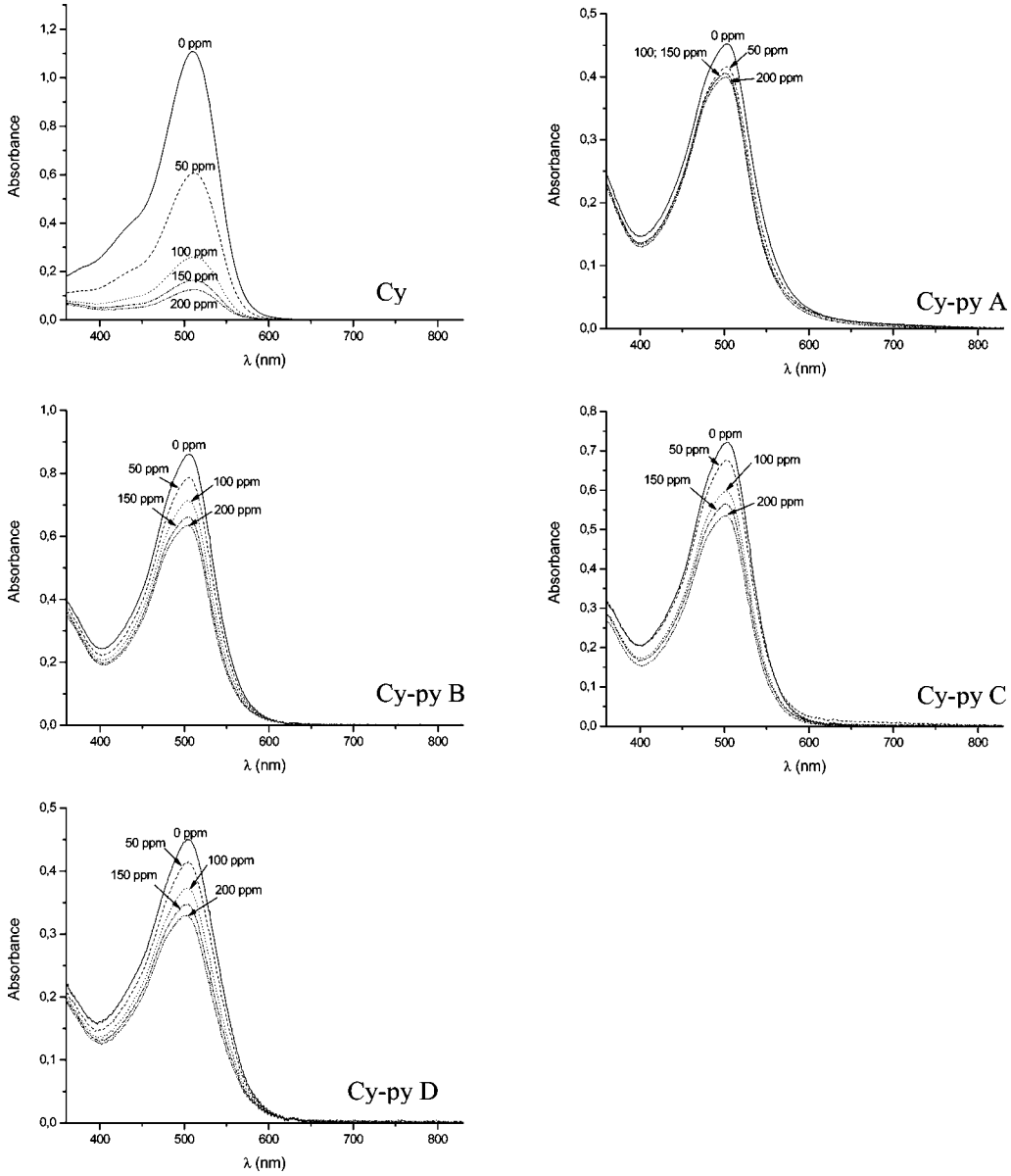

Figure 5. UV/vis spectra of cyanidin-3-*O*-glucoside (Cy-3-glc) and cyanidin–pyruvic acid adducts (Cy-py) A–D at pH 2.0 with increasing amounts of bisulfite (0–200 ppm).

to the doublet (J = 7.7 Hz) at 4.71 ppm. All of the glucosyl protons were situated in the 3.30−3.94 ppm region. The doublet (J = 7.1 Hz) at 4.86 ppm corresponds to the anomeric proton of the second glucosyl moiety. The glucosyl protons were situated in the 3.19−3.90 ppm region. All of the carbons of the sophorosyl moiety were assigned through direct $^{1}H-^{13}C$ correlations in the HSQC spectrum.

Pigment D was found to correspond to the cyanidin-3-*O*-sambubioside−pyruvic acid adduct, as shown in **Figure 3**. The MS data of the pigment detected produced a $[M]^+$ ion at *m*/*z* 649 and a fragment ion $[M-294]^+$ at *m*/*z* 355 corresponding to the loss of the sambubiosyl residue. The structure of this anthocyanin−pyruvic acid adduct was also elucidated by NMR analysis (**Table 4**), similar to the analysis of the former pigments. The major differences concerned the sugar moiety.

Sambubiose is composed by a glucose molecule linked to a xylose molecule by a β-(*1*,*2*) linkage. With respect to the glucosyl moiety, the anomeric proton was assigned to the doublet (J = 7.7 Hz) at 4.78 ppm. All of the glucosyl protons were situated in the 3.17−3.88 ppm region. The doublet (J = 7.7 Hz) at 4.69 ppm corresponds to the anomeric proton of the xylosyl moiety. All of the xylosyl protons were situated in the 3.19−3.64 ppm region. All of the carbons of the sambubiosyl moiety were assigned through direct $^{1}H-^{13}C$ correlations in the HSQC spectrum.

Spectroscopic Stability of the Cyanidin−Pyruvic Acid Adducts. The λ_{max} of the four cyanidin−pyruvic acid adducts A−D in the visible range were situated at 503, 506, 505, and 504 nm, respectively. These values of λ_{max} are hypsochromically shifted when compared with that of cyanidin 3-*O*-glucoside (λ_{max}, 509 nm), in aqueous buffer solution at pH 2 (**Figure 4**). Under these experimental conditions, anthocyanin−pyruvic acid adducts present an orange/red color.

The color displayed by the cyanidin−pyruvic acid adducts was shown to change only slightly with increasing pH up to neutral conditions at which the anthocyanin cyanidin-3-*O*-glucoside is practically all converted into its colorless hemiacetal form (**Figure 4**). This higher resistance to discoloration of anthocyanin−pyruvic acid adducts can be explained by a greater protection of the chromophore moiety against the nucleophilic attack by water to give the respective hemiacetal form. The bathochromic shift observed at higher pH values results from

Table 5. Color Coordinates of the Solutions of 0.08 mM Cyanidin 3-*O*-Glucoside (Cy-3-glc, Reference) and Cyanidin–Pyruvic Acid Adducts (Cy-py) A–D at pH Values of 1.0, 2.0, 5.0, and 7.0

				pH 1.0				
	L^*	$h_{a,b}$	C^*	ΔE^*	ΔL^*	ΔC^*	ΔH^*	$\Delta h_{a,b}$
Cy-3-glc	74.7	23.8	57.0					
Cy-3-glc-py (A)	80.3	21.6	40.5	17.4	5.6	–16.5	–7.24	–2.2
Cy-3-rut-py (B)	73.9	18.7	53.1	6.3	–0.8	–3.9	–2.2	–5.1
Cy-3-soph-py (C)	79.3	18.8	44.3	14.1	4.6	–12.7	–4.27	–5.0
Cy-3-samb-py (D)	84.2	13.9	33.4	26.3	9.7	–23.6	9.44	–9.9
				pH 2.0				
	L^*	$h_{a,b}$	C^*	ΔE^*	ΔL^*	ΔC^*	ΔH^*	$\Delta h_{a,b}$
Cy-3-glc	76.5	22.3	54.3					
Cy-3-glc-py (A)	85.5	30.1	30.7	25.8	9.0	–23.6	–6.68	7.8
Cy-3-rut-py (B)	77.3	28.1	50.8	6.4	0.8	–3.5	0.90	5.8
Cy-3-soph-py (C)	82.7	30.1	41.2	15.9	6.2	–3.5	–2.57	7.8
Cy-3-samb-py (D)	85.1	22.0	31.1	24.8	8.6	–23.2	–1.44	–0.3
				pH 5.0				
	L^*	$h_{a,b}$	C^*	ΔE^*	ΔL^*	ΔC^*	ΔH^*	$\Delta h_{a,b}$
Cy-3-glc	94.8	354.1	6.8					
Cy-3-glc-py (A)	81.9	28.5	34.5	31.9	–12.9	27.7	5.6	–325.6
Cy-3-rut-py (B)	79.4	22.2	38.8	36.3	–15.4	32.0	–6.0	–331.9
Cy-3-soph-py (C)	83.9	25.0	31.8	28.3	–10.9	25.0	–9.3	–329.1
Cy-3-samb-py (D)	87.4	19.9	20.4	16.3	–7.4	13.6	4.1	–334.2
				pH 7.0				
	L^*	$h_{a,b}$	C^*	ΔE^*	ΔL^*	ΔC^*	ΔH^*	$\Delta h_{a,b}$
Cy-3-glc	91.1	319.1	3.6					
Cy-3-glc-py (A)	64.3	18.2	38.7	45.7	–26.8	35.1	4.0	–300.9
Cy-3-rut-py (B)	72.4	11.8	27.3	31.5	–18.7	23.7	–2.8	–307.3
Cy-3-soph-py (C)	78.1	11.4	22.1	23.9	–13.0	18.5	–0.8	–307.7
Cy-3-samb-py (D)	84.8	22.0	13.8	14.1	–6.3	10.2	5.0	–297.1

the equilibrium displacement toward the formation of the quinoidal structures of the cyanidin−pyruvic acid adducts. The nature of the sugar attached to the chromophore seems to be involved in the resistance to nucleophilic attack by water for this kind of pigment. Pigment A has been showed to be less affected than pigments B−D to the pH variations. Nevertheless, equilibrium among different structural forms seems to be slightly different for the cyanidin−pyruvic acid adduct containing a monosaccharide residue (pigment A) than for those of the similar pigments containing disaccharide moieties (pigments B−D) (**Figure 4**). For pigment A, the absorbance intensity at higher pH values corresponding to the pigment quinoidal forms is much higher than that of the lower pH values that corresponds to the flavylium form. In the case of pigments B−D, the absorbance intensities of both forms are similar, with the absorbance intensity of the quinoidal form being less pronounced for pigment D.

All of the cyanidin−pyruvic acid adducts also showed a greater resistance to discoloration by SO_2, when compared with cyanidin-3-*O*-glucoside (**Figure 5**). The decrease in the color intensity of these pigments was small, while the cyanidin-3-*O*-glucoside solution became almost uncolored at the higher concentration of SO_2 (200 ppm). In the anthocyanin structure, the nucleophilic addition of anionic bisulfite occurs at the positively charged C-2 and preferentially at C-4 positions (*33*). In the case of anthocyanin−pyruvic acid adducts, the position C-4 is occupied (ring D), which prevents the nucleophilic attack of bisulfite in that position. The small decrease of the color intensity observed for these pigment solutions can be explained by the nucleophilic attack of bisulfite at the less favored C-2 position of the anthocyanin−pyruvic adduct molecules. These results are in agreement with the respective bleaching constants (K_{SO_2}) calculated. Indeed, the K_{SO_2} obtained for cyanidin-3-*O*-glucoside (4.8×10^{-3}) is 4 or more times higher to those observed for anthocyanin−pyruvic acid adducts (1×10^{-3} or smaller). As observed for the nucleophilic attack by water, the nature of the sugar seems to influence the resistance to the nucleophilic attack by bisulfite. Indeed, anthocyanin−pyruvic acid adducts with glucose or sambubiose attached to the 3-O position of the flavylium moiety (pigments A and D) showed a smaller bleaching constant comparing with similar pigments that possess a rutinosyl or sophorosyl moiety (pigments B and C).

Color Parameters of the Cyanidin−Pyruvic Acid Adducts. All pigments were submitted to $L^*a^*b^*$ color measurements based on the CIELAB colorimetric coordinates L^*, lightness; C^*, chroma; and $h_{a,b}$, hue angle. These studies were carried out at four pH values (1.0, 2.0, 5.0, and 7.0), and the results obtained are summarized in **Table 5**. The colorimetric parameters were expressed by the difference between each solution of cyanidin−pyruvic acid adducts (A−D) and the cyanidin-3-*O*-glucoside solution. These color differences displayed by each cyanidin−pyruvic acid adduct resulting from different substitution models became more evident using cyanidin-3-*O*-glucoside as a reference pigment.

Pigments A−D solutions at pH 2.0 presented higher values of the hue angle ($h_{a,b}$), when compared with pH 1.0, which means that the color of these solutions shifted toward the yellow pole of the chromatic circle, thereby yielding a more orange color. This color difference was easily perceivable in the solutions. For higher pH values, such as 5.0 and 7.0, this trend was reversed and smaller values of the hue angle were obtained, thereby shifting the color of the solution to the blue pole of the chromatic circle.

In the case of the anthocyanin solution (cyanidin-3-*O*-glucoside), this change was not significant and the hue angle at both acidic pH values was similar. For solutions with pH 5.0

and 7.0, a big increase in the hue angle was observed and, thus, a color displacement toward the blue pole of the chromatic circle.

The cyanidin−pyruvic acid adducts (A−D) presented a lower value of the hue angle ($h_{a,b}$) than the cyanidin-3-*O*-glucoside at pH 1.0, 5.0, and 7.0 (**Table 5**). Therefore, at these pH values, the solution hue moves bluer for all pigments (A−D). Curiously, the opposite trend was observed at pH 2.0 (**Table 5**), where the pyruvic acid adducts revealed a higher hue angle ($h_{a,b}$) than cyanidin-3-*O*-glucoside (except for pigment D), contributing to yellower solutions at this pH (for all pigments, except D).

In comparison of pigments A−D and the anthocyanin cyanidin-3-*O*-glucoside at both acidic pH values (1.0 and 2.0) (**Table 5**), the solutions of pigment A−D are less saturated than the reference solution, which is revealed by the negative difference chroma value ($C^* < 0$) obtained (**Table 5**). On the other hand, all pigment solutions presented higher lightness values (L^*), comparative to the reference (except pigment B at pH 1), which reveals an increase of the lightness of the respective solutions. Because color intensity is related to lightness and chroma, the loss of saturation ($\Delta C^* < 0$) and the increase of lightness ($\Delta L^* > 0$) presented by the cyanidin−pyruvic acid adduct solutions showed that they are much less colored than the cyanidin-3-*O*-glucoside. For higher pH values (5.0 and 7.0), the reverse trend was observed and these solution revealed an increase in the saturation ($\Delta C^* > 0$) and a decrease in the lightness ($\Delta L^* > 0$), when compared to the reference (cyanidin-3-*O*-glucoside). Perceptually, this means that these pigments (except B) have a much lower color strength than cyanidin-3-*O*-glucoside at more acidic pH values (1.0 and 2.0). In other hand, for pH values of 5.0 and 7.0, the cyanidin−pyruvic acid adduct studied are much more colored than the anthocyanin.

ΔE^* represents the global color difference between the different anthocyanin−pyruvic acid adducts and the cyanidin-3-*O*-glucoside (reference), and ΔE^* calculation showed that, at pH values of 1.0 and 2.0, the smallest ΔE^* is observed in both cases and by a far margin with the rutinosyl derivative (pigment B). For the higher pH values studied, the smallest ΔE^* is observed for the sambubiosyl derivative (pigment D).

Color changes resulting by the presence of different sugars in the anthocyanin−pyruvic acid adduct moiety affected the three parameters of color: chroma (C^*), lightness (L^*), and hue angle ($h_{a,b}$). In general, the solutions of anthocyanin−pyruvic acid adducts containing a monosaccharide moiety (pigment A) presented a higher $h_{a,b}$ value when compared to the solution of the anthocyanin−pyruvic acid adduct containing a disaccharide (B−D), which means that the chromatic tonality of the solutions shifted to a more orange hue. The anthocyanin−pyruvic acid adduct containing a disaccharide (except pigment D) also showed higher chroma and lower lightness values, which reveals an increase of the color intensity of these solutions, comparative to cyanidin−pyruvic acid adducts containing a monosaccharide moiety.

Overall, the color characteristics of these pigments, namely, the color stability at a wide pH range and the high resistance to bleaching by bisulfite, as well as the higher coloring capacity of these pigments with the increasing pH, are important features, indicating a putative application of these compounds in food products. Nevertheless, further studies will be performed, especially regarding their stability directly in food matrixes.

LITERATURE CITED

(1) Brouillard, R. Chemical structure of anthocyanins. In *Anthocyanins as Food Colors*; Markakis, P., Ed.; Academic Press, Inc.: New York, 1982; pp 1−38.

(2) von Elbe, J. H.; Schwartz, S. J. Colorants. In *Food Chemistry*, 3rd ed.; Fennema, O. R., Ed.; Marcel Dekker, Inc.: New York, 1996; pp 651−723.

(3) Somers, T. C. The polymeric nature of red pigments. *Phytochemistry* **1971**, *10*, 2175−2186.

(4) Timberlake, C. F.; Bridle, P. Interactions between anthocyanins, phenolic compounds and acetaldehyde and their significance in red wines. *Am. J. Enol. Vitic.* **1976**, *27*, 97−105.

(5) Vivar-Quintana, A. M.; Santos-Buelga, C.; Francia-Aricha, E.; Rivas-Gonzalo, J. C. Formation of anthocyanin-derived pigments in experimental red wines. *Food Sci. Technol. Int.* **1999**, *5*, 347−352.

(6) Jurd, L.; Somers, T. C. The formation of xanthylium salt from proanthocyanidins. *Phytochemistry* **1970**, *9*, 419−427.

(7) Santos-Buelga, C.; Bravo-Haro, S.; Rivas-Gonzalo, J. C. Interactions between catechin and malvidin-3-monoglucoside in model solutions. *Z. Lebensm.-Unters. Forsch. A* **1995**, 269−274.

(8) Liao, H.; Cai, Y.; Haslam, E. Polyphenols interactions. Anthocyanins: Copigmentation and color changes in red wines. *J. Sci. Food Agric.* **1992**, *59*, 299−305.

(9) Remy, S.; Fulcrand, H.; Labarbe, B.; Cheynier, V.; Moutounet, M. First confirmation in red wines of products resulting from direct anthocyanin−tannin reactions. *J. Sci. Food Agric.* **2000**, *80*, 745−751.

(10) Rivas-Gonzalo, J. C.; Bravo-Haro, S.; Santos-Buelga, C. Detection of compounds formed through the reaction of malvidin 3-monoglucoside and catechin in the presence of acetaldehyde. *J. Agric. Food Chem.* **1995**, *43*, 1444−1449.

(11) Bakker, J.; Timberlake, C. F. Isolation, identification, and characterization of new color-stable anthocyanins occurring in some red wines. *J. Agric. Food Chem.* **1997**, *45*, 35−43.

(12) Fulcrand, H.; Benabdeljalil, C.; Rigaud, J.; Cheynier, V.; Moutounet, M. A new class of wine pigments generated by reaction between pyruvic acid and grape anthocyanins. *Phytochemistry* **1998**, *47*, 1401−1407.

(13) Mateus, N.; Silva, A. M. S.; Vercauteren, J.; de Freitas, V. Occurrence of anthocyanin-derived pigments in red wines. *J. Agric. Food Chem.* **2001**, *49*, 4836−4840.

(14) Benabdeljalil, C.; Cheynier, V.; Fulcrand, H.; Hakiki, A.; Mosaddak, M.; Moutounet, M. Mise en évidence de nouveaux pigments formés par réaction des anthocyanes avec des métabolites de levures. *Sci. Aliments* **2000**, *20*, 203−220.

(15) Mateus, N.; de Freitas, V. A. P. Evolution and stability of anthocyanin-derived pigments during Port wine aging. *J. Agric. Food Chem.* **2001**, *49*, 5217−5222.

(16) Bakker, J.; Bridle, P.; Honda, T.; Kuwano, H.; Saito, N.; Terahara, N.; Timberlake, C. Isolation and identification of a new anthocyanin occurring in some red wines. *Phytochemistry* **1997**, *44*, 1375−1382.

(17) Mateus, N.; Pascual-Teresa, S.; Rivas-Gonzalo, J. C.; Santos-Buelga, C.; de Freitas, V. Structural diversity of anthocyanin-derived pigments in port wines. *Food Chem.* **2002**, *76*, 335−342.

(18) Francia-Aricha, E. M.; Guerra, M. T.; Rivas-Gonzalo, J. C.; Santos-Buelga, C. New anthocyanin pigments formed after condensation with flavanols, *J. Agric. Food Chem.* **1997**, *45*, 2262−2266.

(19) Romero, C.; Bakker, J. Interactions between grape anthocyanins and pyruvic acid, with effect of pH and acid concentration on anthocyanin composition and color in model solutions. *J. Agric. Food Chem.* **1999**, *47*, 3130−3139.

(20) Sarni-Manchado, P. S.; Fulcrand, H.; Souquet, J. M.; Cheynier, V.; Moutounet, M. Stability and color of unreported wine anthocyanin-derived pigments. *J. Food Sci.* **1996**, *61*, 938−941.

(21) Pissarra, J.; Mateus, N.; Rivas-Gonzalo, J. C.; Santos-Buelga, C.; de Freitas, V. A. P. Reaction between malvidin 3-glucoside and (+)-catechin in model solutions containing different aldehydes. *J. Food Sci.* **2003**, *68*, 476−481.

(22) Bax, A.; Subramanian, S. Sensitivity enhanced two-dimensional heteronuclear shift correlation NMR spectroscopy. *J. Magn. Res.* **1986**, *67*, 565−569.

(23) Bax, A.; Summers, M. F. ^{1}H and ^{13}C assignments from sensitivity-enhanced detection of heteronuclear multiple-bond connectivity by 2D multiple quantum NMR. *J. Am. Chem. Soc.* **1986**, *108*, 2093−2094.

(24) Robinson, R. A.; Stokes, R. H. *Electrolyte Solutions, the Measurement and Interpretation of Conductance, Chemical Potential, and Diffusion in Solutions of Simple Electrolytes*, 2nd ed.; Butterworths: London, U.K., 1968.

(25) CIE. *Colorimetry*, 2nd ed.; Publication 15-2; Central Bureau of the CIE: Vienna, Austria, 1986.

(26) Gonnet, J. F. Color effects of co-pigmentation of anthocyanin revisited−b1. A colorimetric definition using the CIELAB scale. *Food Chem.* **1998**, *63*, 409−415.

(27) Gonnet, J. F. Color effects of co-pigmentation of anthocyanin revisited−2. A colorimetric look at the solutions of cyanin co-pigmented by rutin using CIELAB scale. *Food Chem.* **1999**, *66*, 387−394.

(28) Gao, L.; Mazza, G. Characterisation, quantification, and distribution of anthocyanins and colorless phenols in cherries. *J. Agric. Food Chem.* **1995**, *43*, 343−346.

(29) Bridle, P.; García-Viguera, C. Analysis of anthocyanins in strawberries and elderberries. A comparison of capillary zone electrophoresis and HPLC. *Food Chem.* **1997**, *59*, 299−304.

(30) Mullen, W.; Lean, M. E. J.; Crozier, A. Rapid characterization of anthocyanins in red raspberry fruit by high-performance liquid chromatography coupled to single-quadrupole mass spectrometry. *J. Chromatogr., A* **2002**, *966*, 63−70.

(31) Barritt, B. H.; Torre, L. C. Cellulose thin-layer chromatography separation of *Rubus* fruit anthocyanins. *J. Chromatogr., A* **1973**, *75*, 151−155.

(32) Spanos, G. A.; Wrolstad, R. E. Anthocyanin pigment, nonvolatile acid, and sugar composition of red raspberry juice. *J. Assoc. Off. Anal. Chem.* **1987**, *70*, 1036.

(33) Berké, B.; Chèze, C.; Vercauteren, J.; Deffieux, G. Bisulfite addition to anthocyanins: Revisited structures of colorless adducts. *Tetrahedron Lett.* **1998**, *39*, 5771−5774.

Received for review April 18, 2006. Revised manuscript received June 30, 2006. Accepted June 30, 2006. The authors thank the Portugal−Spain Programme of "Acciones integradas" for the financial support to the mobility of researchers (references HP01-24 and E-23/02). This research was supported by a grant from FCT (Fundação para a Ciência e a Tecnologia−Praxis BD/22622/2005), by a grant from Ministério da Agricultura (P.O. AGRO 386), both from Portugal, and by FEDER funding.

JF061085B